Impinging buoyant plumes

ÉCOLE CENTRALE LYON

LMFA

Imperial College London

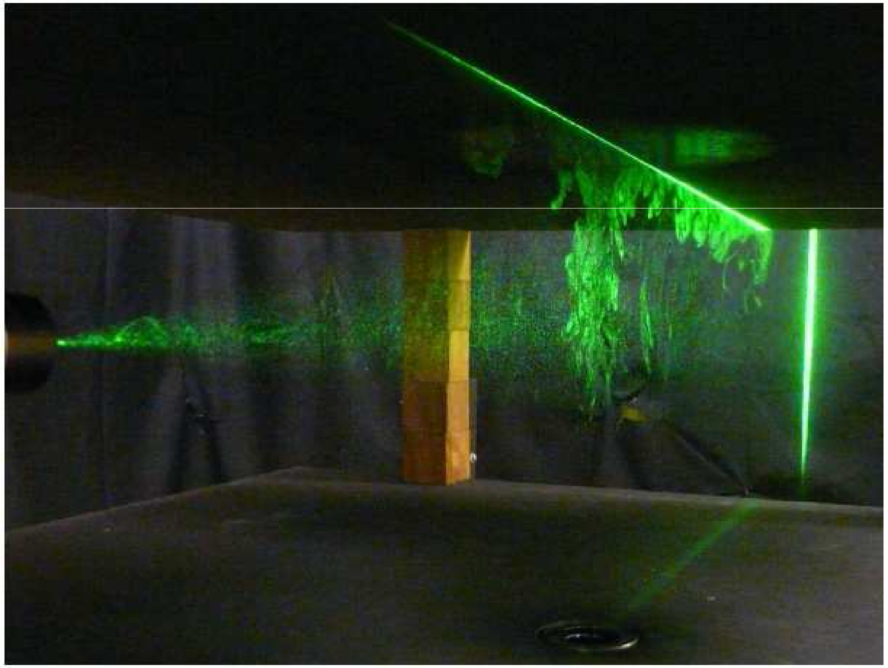

Adam Ezzamel, **Pietro Salizzoni**, Gary Hunt

Context:
Early filling box transients

KAYE, N. B. & HUNT, G. R. 2007 Overturning in a filling box. *J. Fluid Mech.* **576**, 297–323.

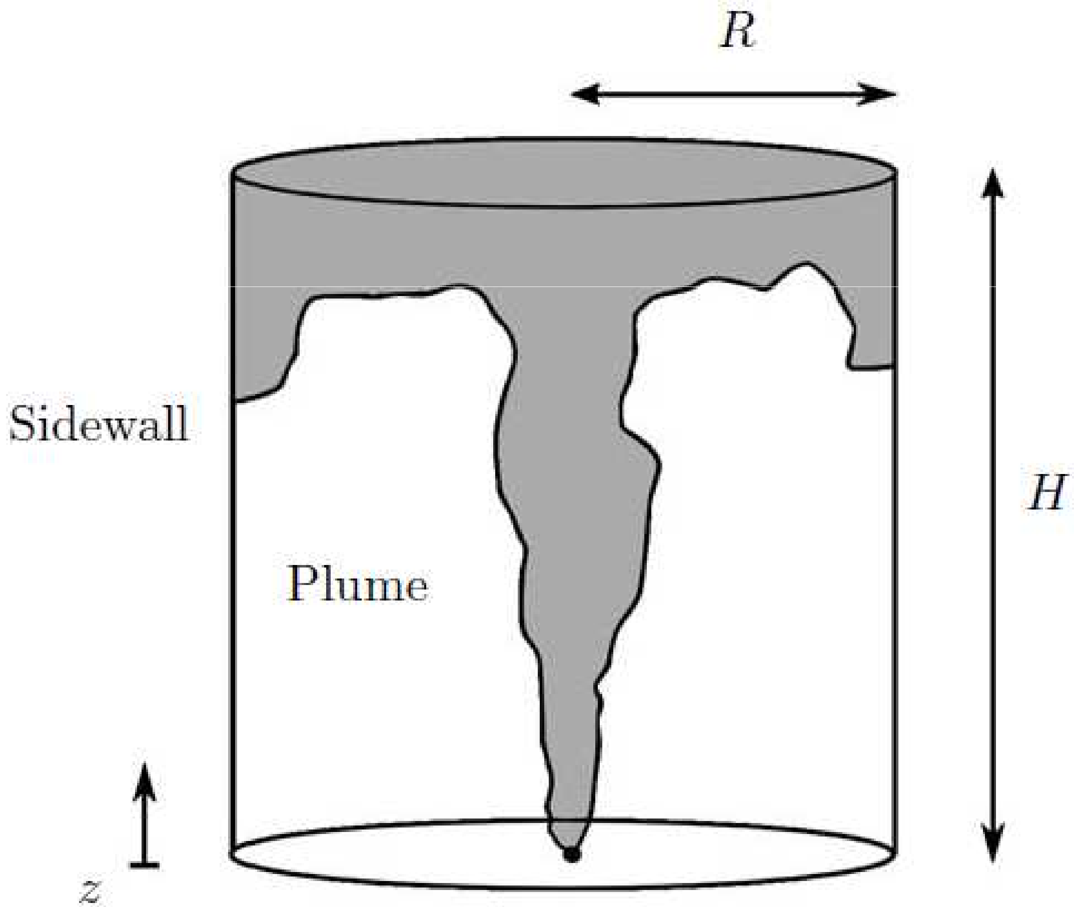

Context:
Early filling box transients

Kaye, N. B. & Hunt, G. R. 2007 Overturning in a filling box. *J. Fluid Mech.* **576**, 297–323.

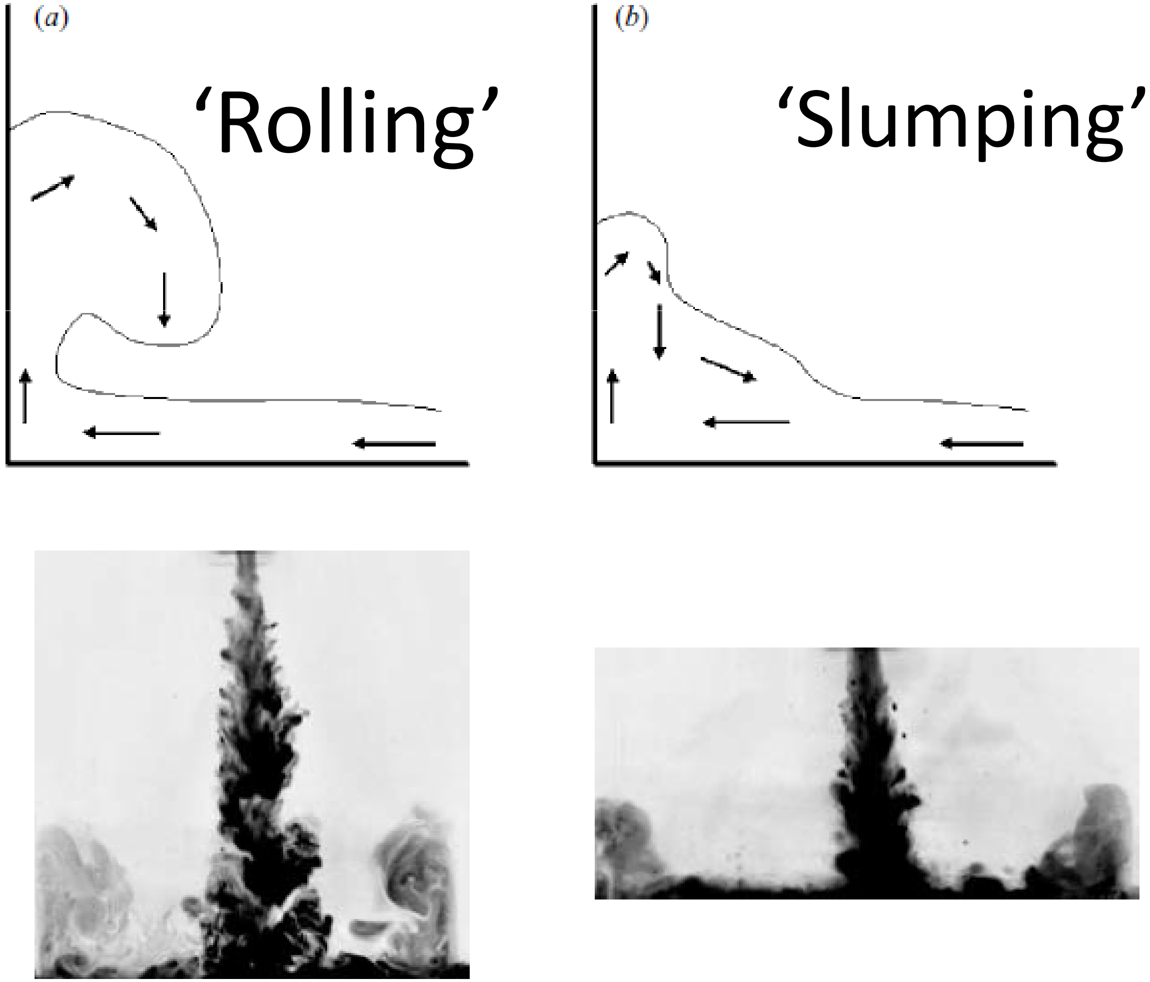

Impinging turbulent plumes

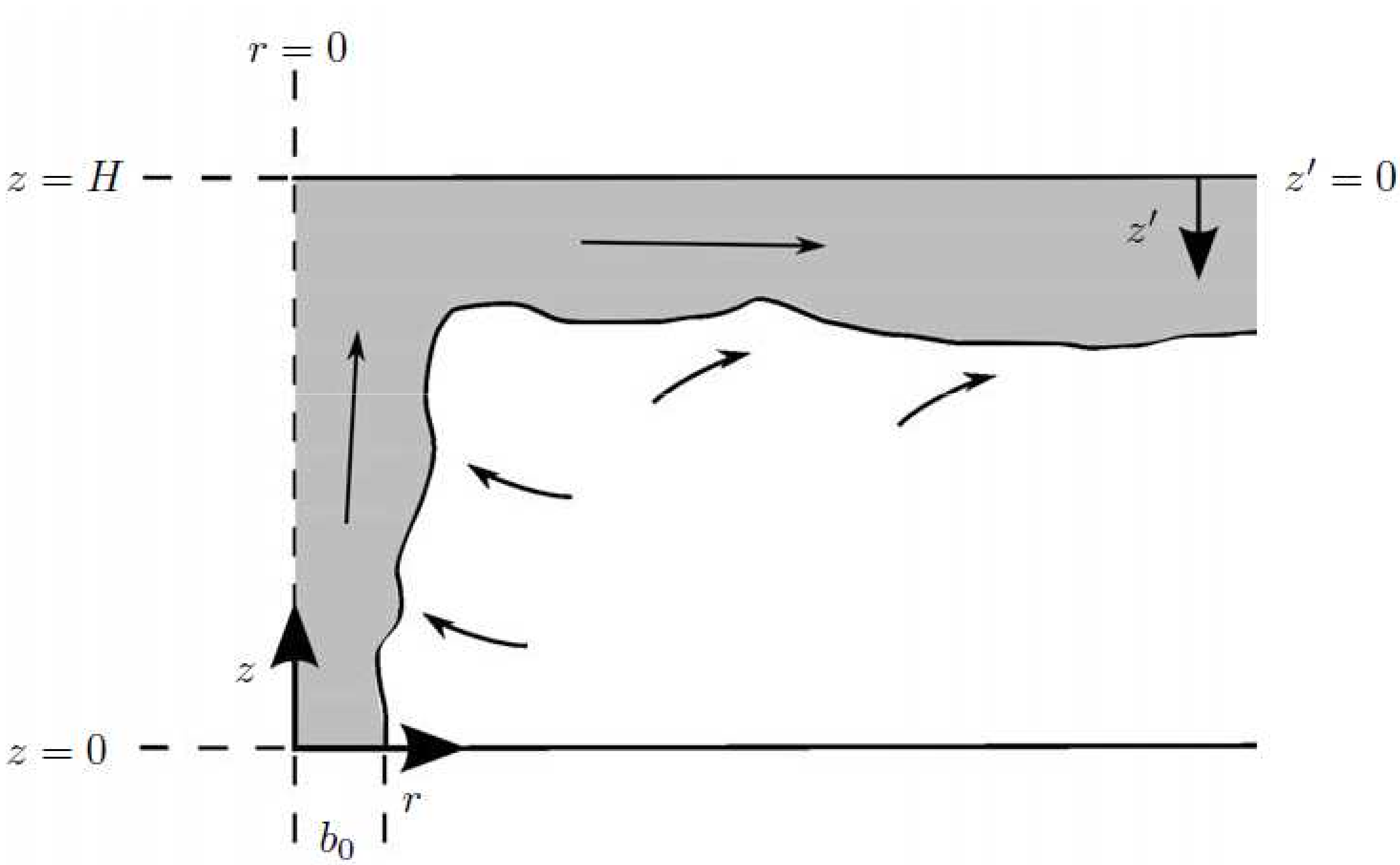

Objectives of study

1. Investigate velocity profiles / turbulence dynamics
2. Evaluate dynamic head loss at impingement
3. Buoyancy / momentum balance in radial flow
4. Estimate entrainment coefficient

Experiment

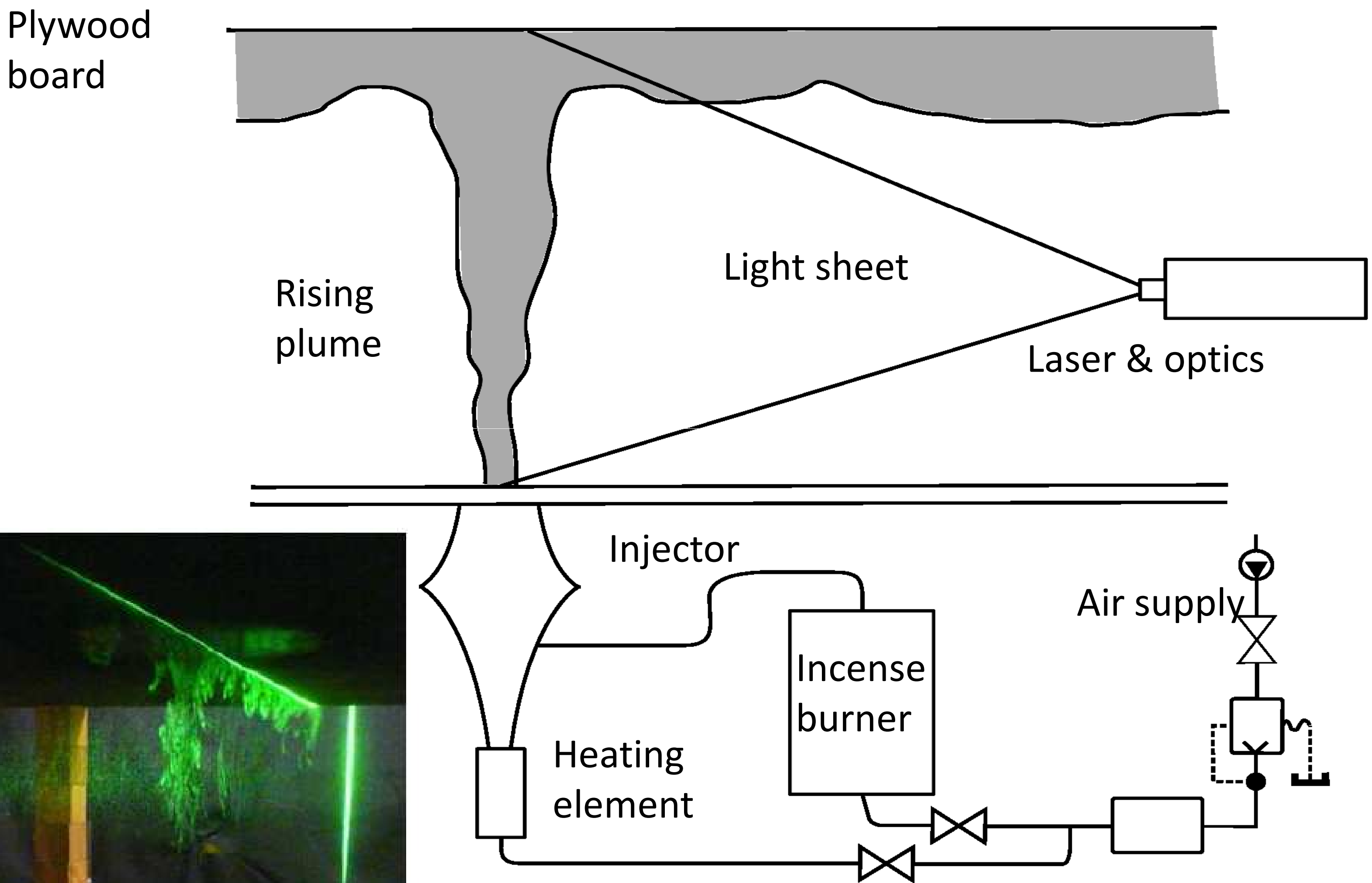
Plywood
board
Rising
plume
Light sheet
Laser & optics
Injector
Air supply
Incense
burner
Heating
element

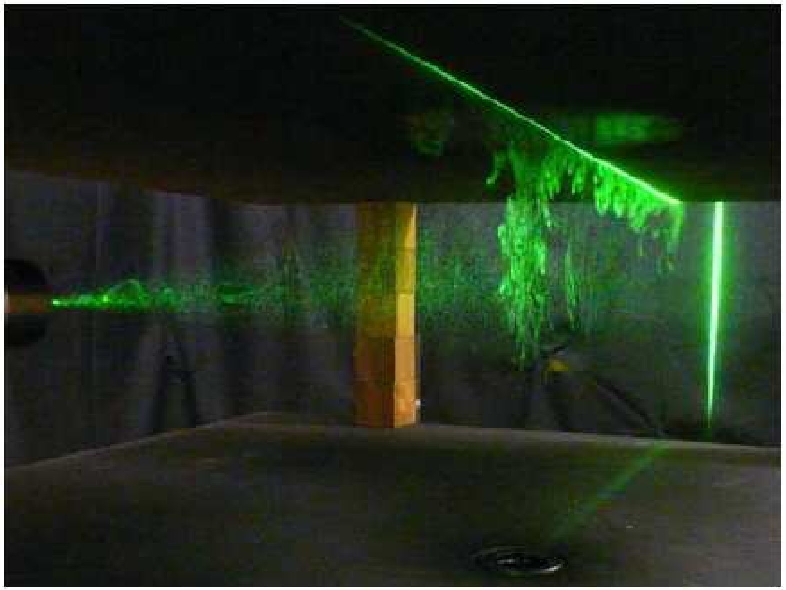

Measurement techniques

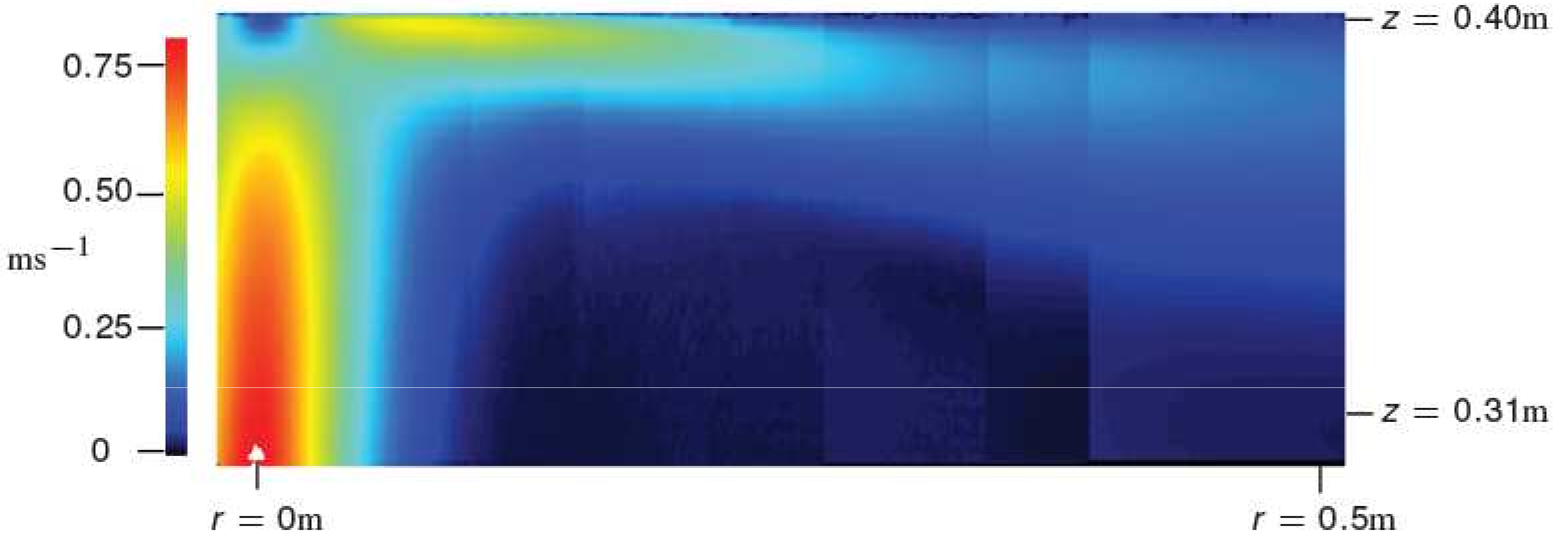

- Air heated to 100℃.
- Nozzle diaphragms used to change source condition.
- Exit velocity 0.4 - 18 m/s
- Measurements with PIV, thermocouples

Impinging turbulent plumes

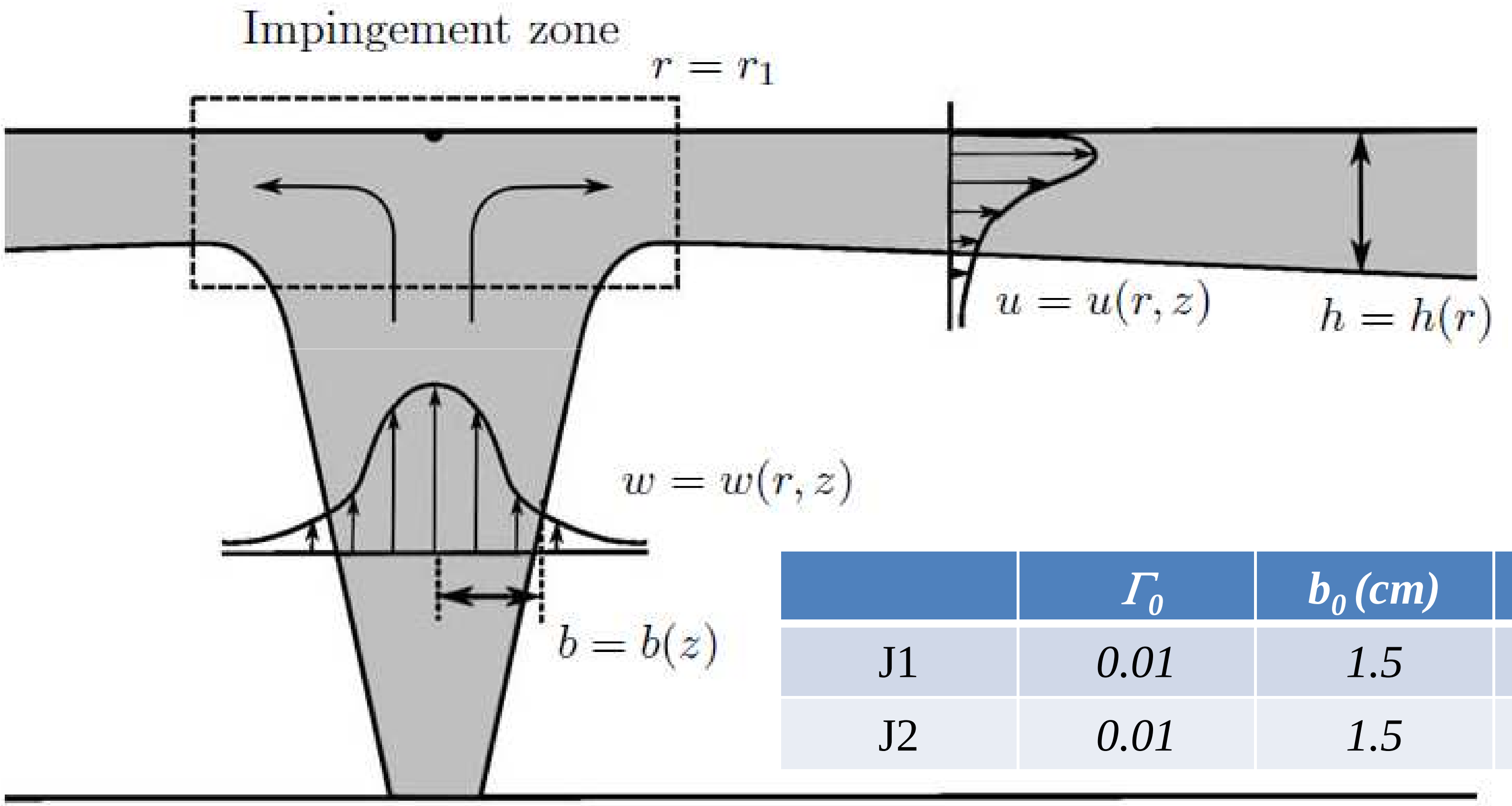

	Γ_0	b_0 (cm)	H(m)
J1	0.01	1.5	0.4
J2	0.01	1.5	0.6

$$\Gamma(z) = \frac{5}{2^{7/2}\pi^{1/2}\alpha}\frac{Q(z)^2 B(z)}{M(z)^{5/2}}$$

Radial velocity profile

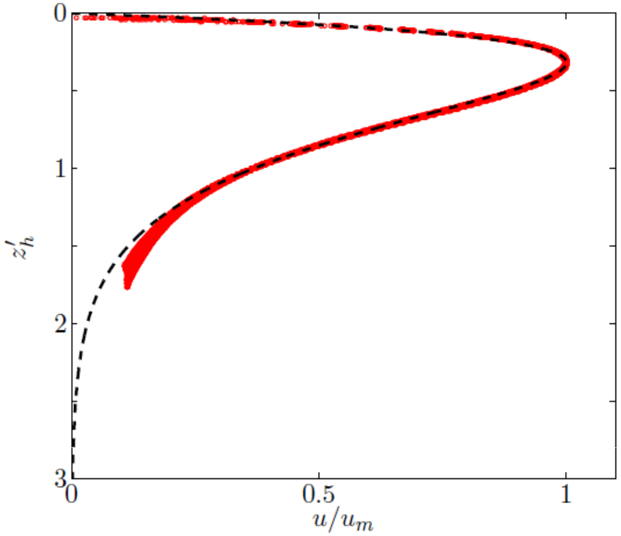

$$u(r,z') = \mu_2(r)\, z' \exp\left(\frac{-z'}{\sigma_2(r)}\right)$$

$$\frac{u}{u_m(r)} = \pi \frac{z'}{h_u(r)} \exp\left(1 - \frac{\pi z'}{h_u(r)}\right)$$

Very good fit of this functional form

Buoyancy profile

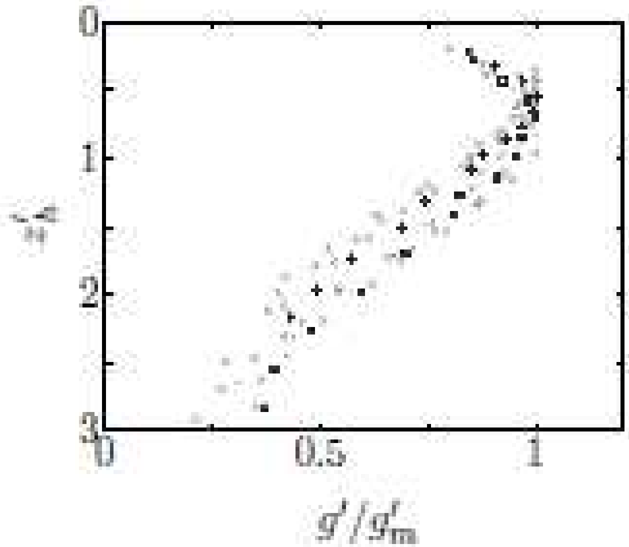

Non-buoyant jet
Separation

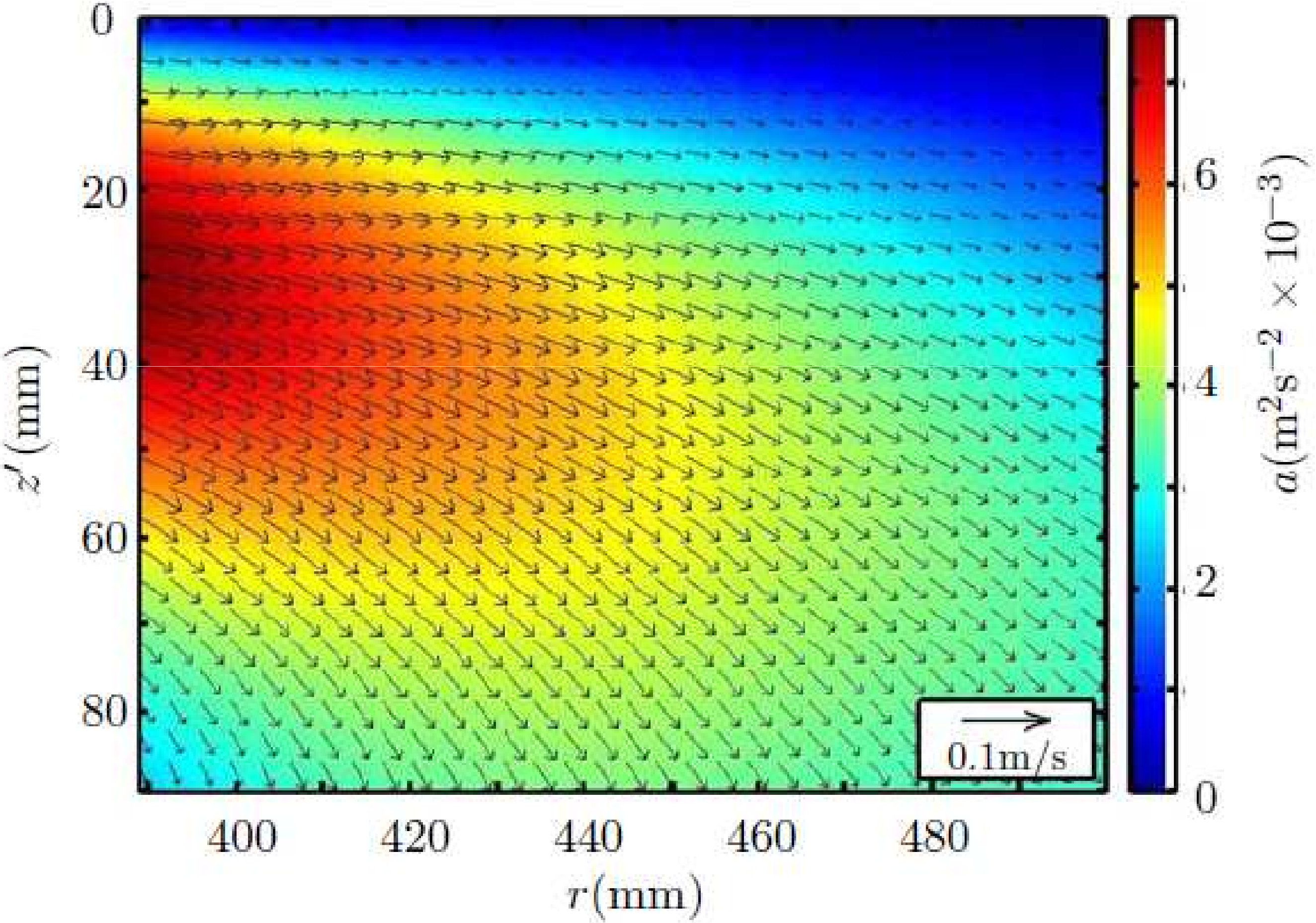

Buoyant

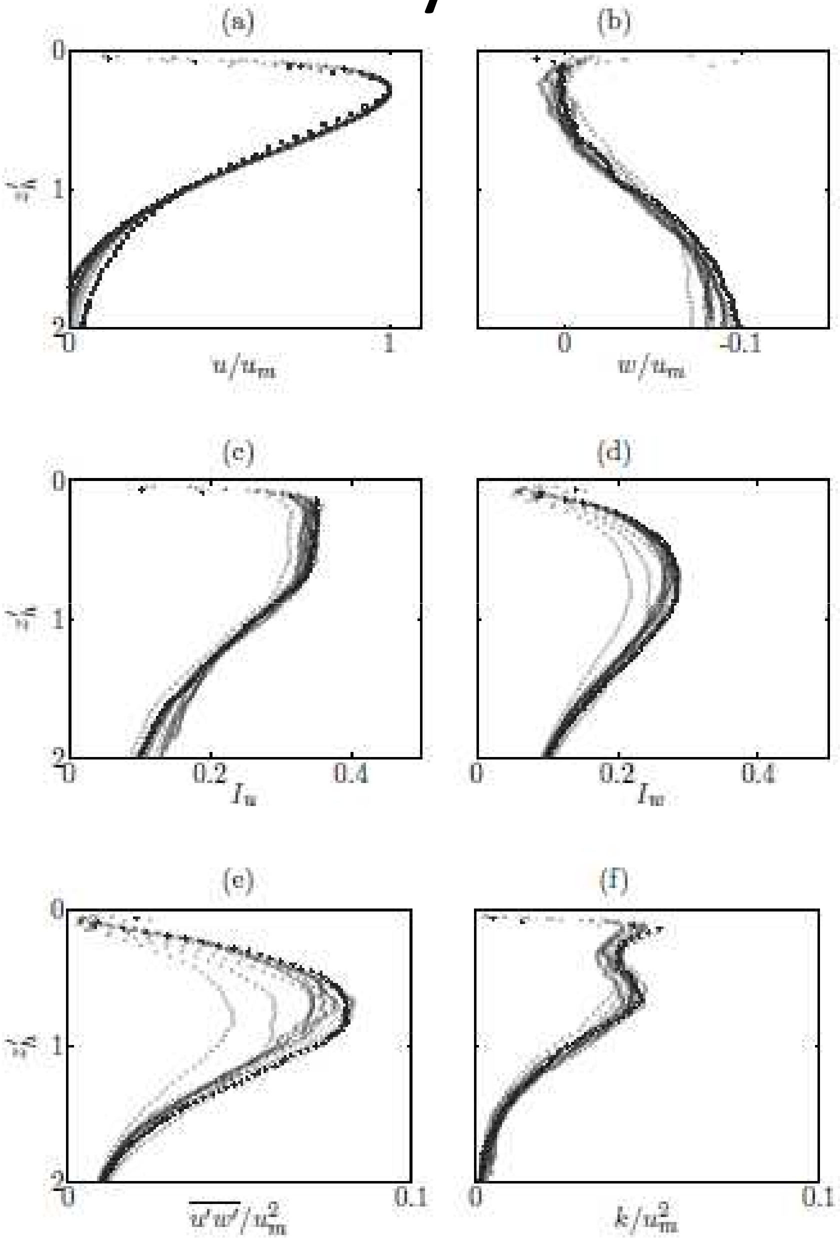

Non-Buoyant

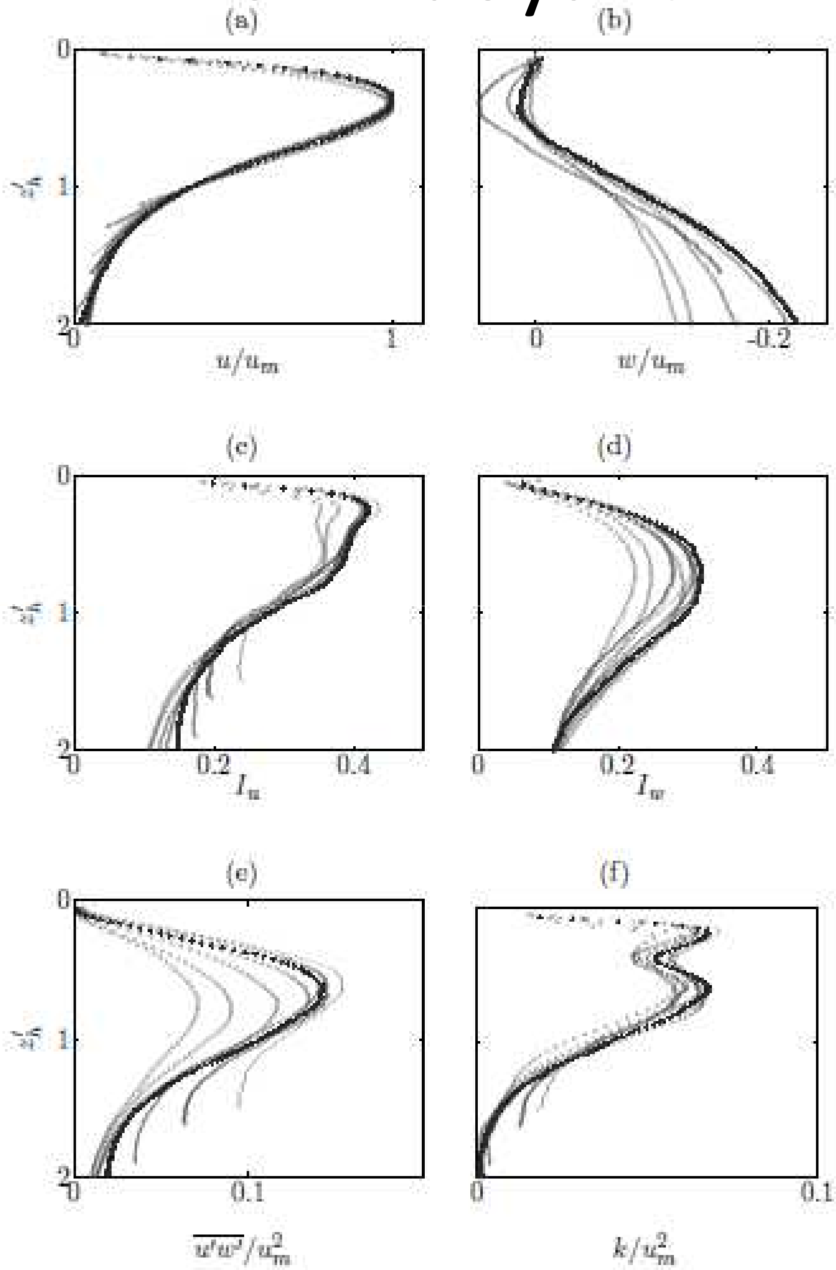

Dynamic head loss coefficient

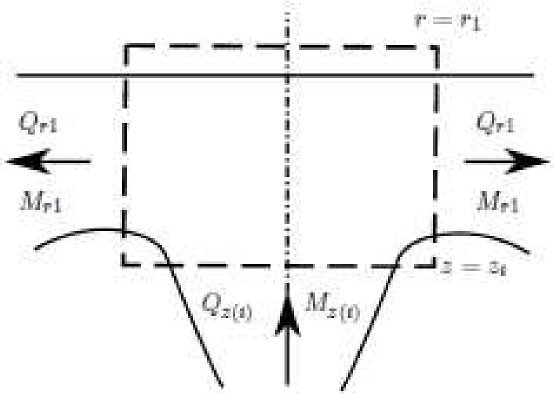

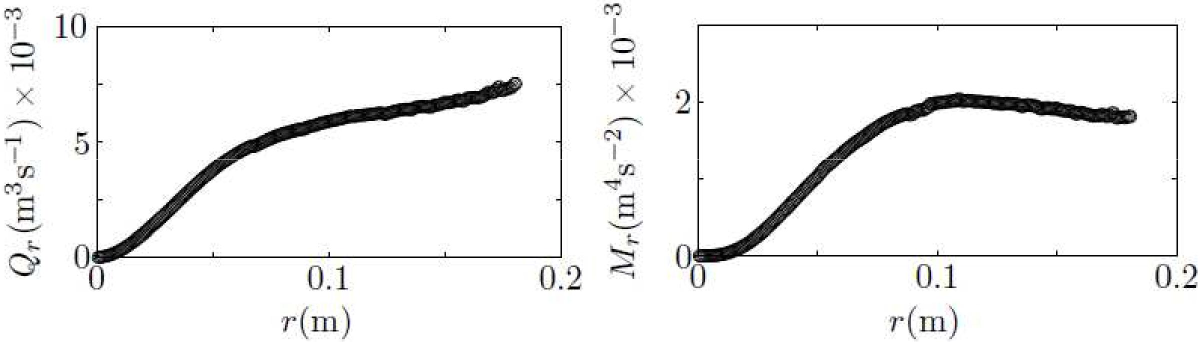

(b) (d)

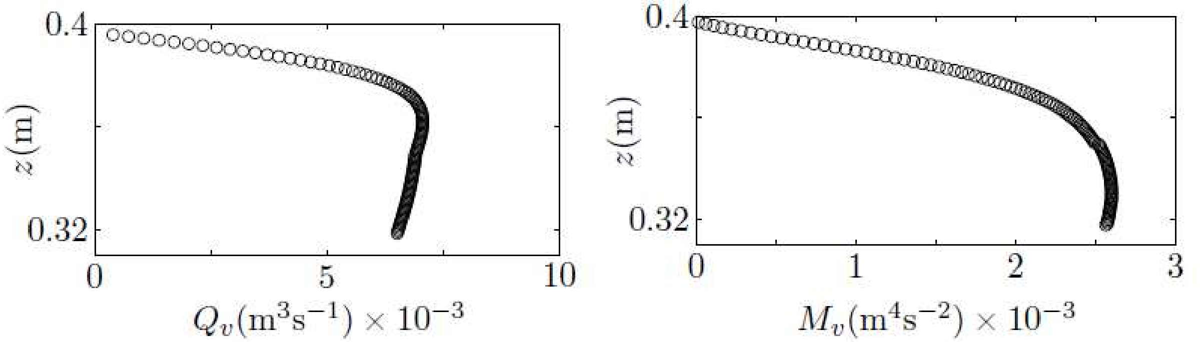

$$\gamma = \frac{M_{r1}}{M_{vi}}$$

$$\gamma = 0.80$$

Momentum – buoyancy balance

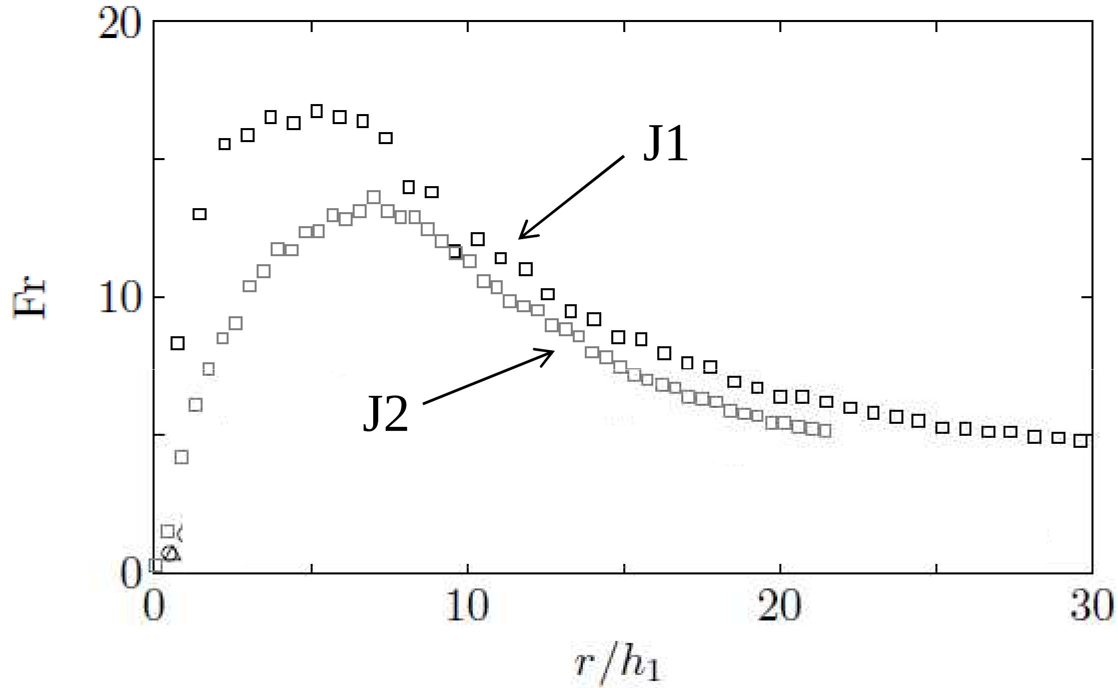

$$Fr = \frac{\bar{u}}{\sqrt{gh}}$$

Outflow initially momentum-dominated plumes

Entrainment coefficient

$$\frac{1}{r}\frac{d}{dr}(ruh) = \varepsilon u$$

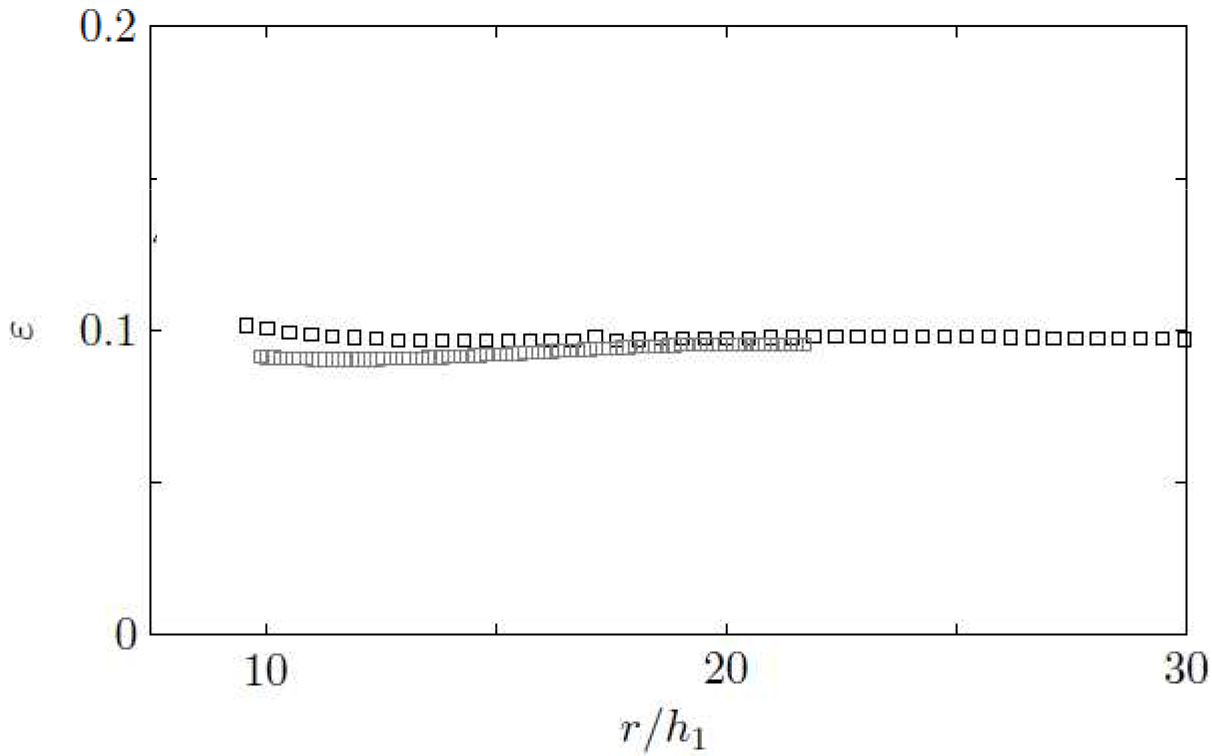

Comparison with an integral model

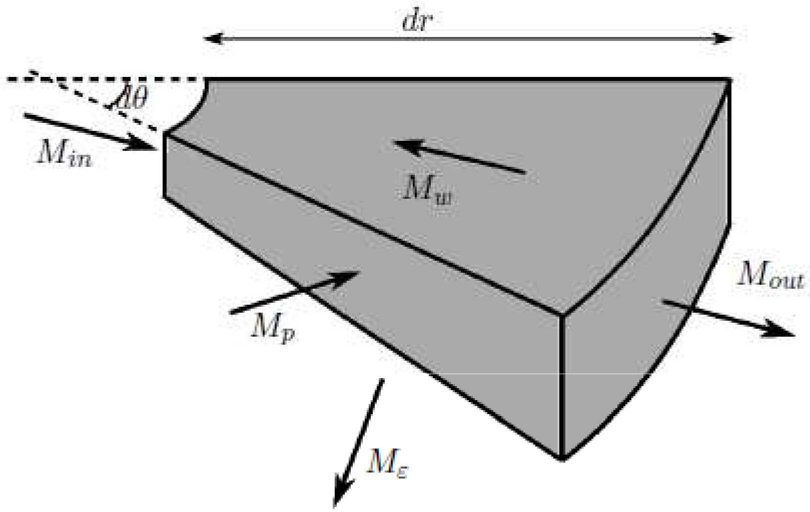

$$\begin{cases} \frac{1}{r}\frac{d}{dr}(ruh) = \varepsilon u \\ \frac{d}{dr}(ru^2 h) + \left(\frac{1}{\mathrm{Fr}_1}\right)^2 \frac{r}{2}\frac{d}{dr}(g' h^2) = -ru^2(\varepsilon + C_f) \\ \frac{1}{r}\frac{d}{dr}(rug' h) = -ug' K \end{cases}$$

$$\begin{cases} C_f = \frac{\tau_{wall}}{\rho u^2}. \\ K = C_f \mathrm{Pr}^{-2/3} \end{cases}$$

J1

J2

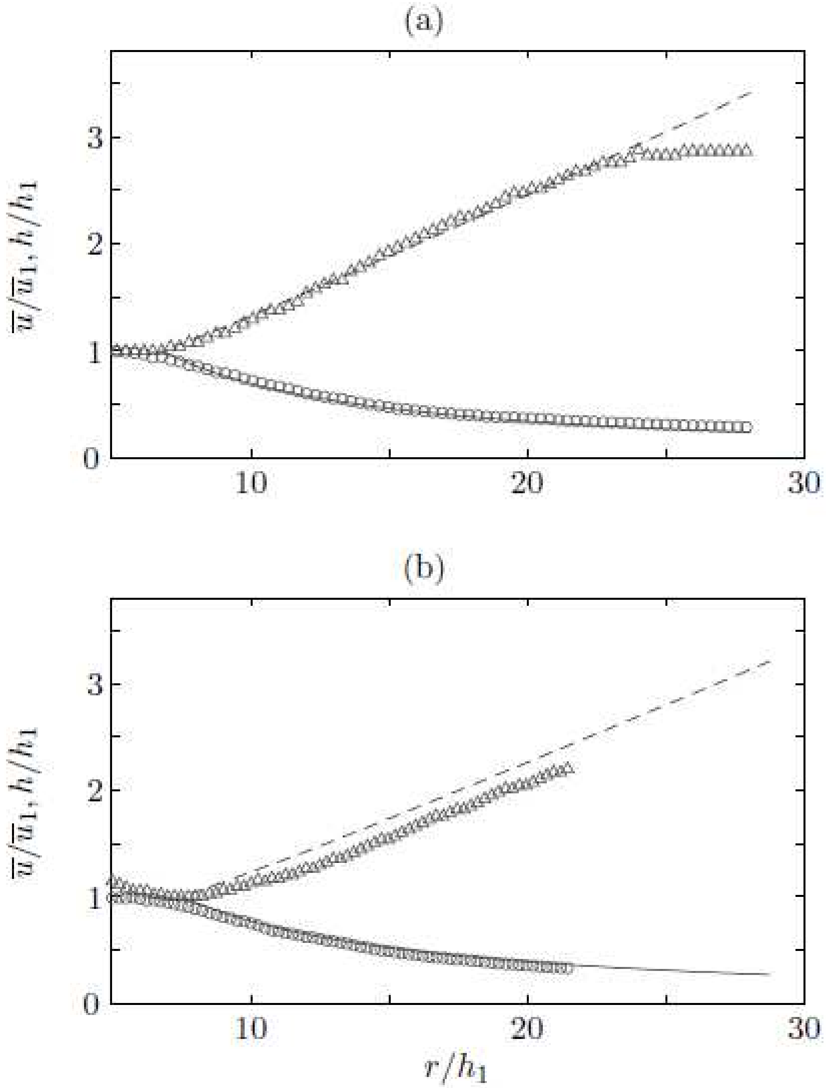

Comparison of experimental measurements with solutions of wall-jet equation for experiments (a) F1 and (b) J2. △ and ○ denote measured h and $\overline{u}$; - - - and — the model solution subject to the parameters listed in table 5.5.

Buoyancy losses

$$B(r) = 2\pi \int_0^h U(r,z)\, g'(r,z)\, r\, dz$$

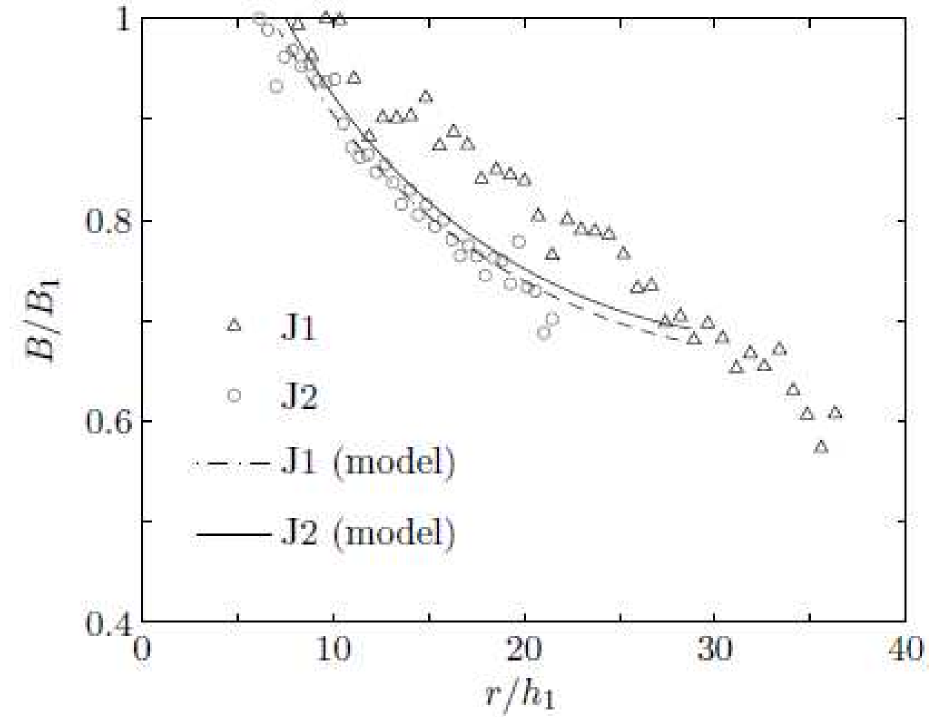

Radial evolution of normalised buoyancy flux B/B_1 in the radial buoyant wall-jet. Point symbols denote experimental data; lines denote solutions to the wall-jet equations (5.13) with $K = C_f = 0.02$.

Concluding remarks

- Outflow initially momentum dominated
- Self-similarity quickly reached
- Experiments and integral models show good agreement
- Entrainment coefficient measured - no systematic *Ri* dependence

Perspectives

- Comparison with LES simulations
- Influence of the unsteady dynamics of the gravity